

# SELF-CONSISTENT INJECTION PAINTING FOR SPACE CHARGE MITIGATION \*

N. J. Evans<sup>†</sup>, A. Hoover, T. Gorlov, V. Morozov, Oak Ridge National Lab, Oak Ridge, TN, USA

## Abstract

The {2,2}-Danilov distribution, or simply the *Danilov* distribution, has a uniform charge distribution, elliptical projections, and can be created by uniformly filling one transverse mode of a coupled ring. In addition to proposing the distribution as an example of beam distribution with linear space charge that satisfies the Vlasov equation, Danilov showed how such a distribution could be constructed using a sufficiently flexible charge exchange injection system, such as at the Spallation Neutron Source (SNS). In this paper we will outline some of the proposed applications of this distribution, provide an update on our attempts to paint one in the SNS ring using a scheme we refer to as ‘eigenpainting’, and discuss some open questions pertaining to the study of this distribution.

## INTRODUCTION

The Danilov distribution, defined in Ref. [1], or simply the *Danilov* distribution offers an opportunity to create a beam with several properties of interest for high brightness beams. Because of the linear nature of the space charge, a Danilov distribution can be matched to a lattice and the resulting system is linear, similar to the K-V distribution [2]. Danilov realized that the correlations present in the distribution imply that it can be built-up successively over many turns by the process of phase space painting [1]. This makes the distribution scalable to more intense beams, not limited by the source, such as another similar distribution described by Liuten [3].

Controlling the speed at which a given footprint is filled allows control of the space charge, offering an interesting opportunity to study a distribution with a relatively tractable description over an easily tunable range of space charge. At SNS we are attempting to paint such a distribution in the accumulator ring to study the properties of these beams. To differentiate from existing painting where both modes of a (typically uncoupled) lattice are filled with amplitudes increasing together, correlated painting, or one amplitude increasing while the other decreases, uncorrelated painting, we refer to painting into a single mode as *eigenpainting*. Note that in the case of uncorrelated painting, the resulting

distribution would be a K-V if it could be maintained in the presence of space charge during the painting process.

The benefits of a Danilov distribution fall into several categories due to: linear space charge, low 4D emittance, and non-zero angular momentum. The last two of these are directly related to the fact that a uniform distribution of charge occupying one of two counter-rotating coupled modes is a Danilov distribution.

Because a properly matched Danilov distribution is a uniformly filled coupled mode with small emittance in the second mode, many of the arguments about possible applications in Refs. [4,5] hold. Notably for space charge mitigation, Burov suggests the use of circular modes for low-energy machines to preserve brightness and reduce tune shift since the larger of the two mode emittances determines to the real space distribution, allowing the other to be made arbitrarily small. For this purpose eigenpainting alone is beneficial without the further constraint of uniform charge density.

However, because the incoherent space-charge tune footprint vanishes for uniform charge distribution, while the tune shift remains, one can imagine a scenario where the tune footprint is compact enough, and the shift large enough that the beam hops over a resonance and resides on the other side of the line without operationally significant loss. There will still be a tail, that still crosses the resonance, but it should be much sparser than that of a Gaussian beam of similar dimensions, as only those particles near the edge of the distribution will experience non-linear forces. Whether this tail is sparse enough to allow this scheme to work is a question we plan on investigating in future simulations and experiments.

Additionally, Cheon et al. have done work investigating whether rotating beams could help reduce the effect of space charge driven resonances [6]. They considered resonances in linacs, which would require either pre-painting beam in a purpose-built low energy ring, or another method of preparation.

The rest of this manuscript will give a brief outline of the setup and techniques used for eigenpainting experiments at SNS and present recent results.

## EXPERIMENTS AT THE SNS

The SNS consists of a 1.0 GeV H<sup>-</sup> linac, which is currently being upgraded to 1.3 GeV, a 248 m accumulation ring equipped with first and second harmonic bunching RF cavities. Figure 1 shows the end of the linac, the ring, and Ring-Target Beam Transport (RTBT) line with relevant features identified.

Injection from the linac to the ring takes place via charge exchange injection facilitated by a thin nano-crystalline diamond foil. Phase space painting is achieved with a set of

\* This manuscript has been authored by UT-Battelle, LLC, under Contract No. DE-AC05-00OR22725 with the U.S. Department of Energy. The United States Government retains, and the publisher, by accepting the article for publication, acknowledges that the United States Government retains a non-exclusive, paid-up, irrevocable, world-wide license to publish or reproduce the published form of this manuscript, or allow others to do so, for United States Government purposes. The Department of Energy will provide public access to these results of federally sponsored research in accordance with the DOE Public Access Plan (<http://energy.gov/downloads/doe-public-access-plan>).

<sup>†</sup> nhe@ornl.gov

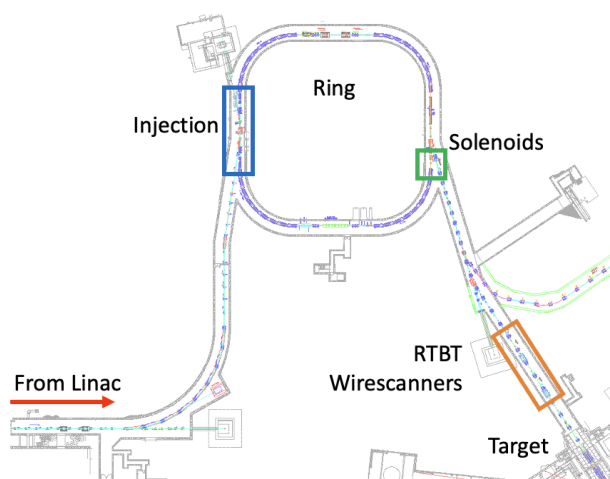


Figure 1: Layout of the SNS ring.

eight time-varying kickers [7], four in each plane, capable of modifying both the position and angle of the closed orbit at the location of the foil throughout the 1 ms long injection process to change the injection coordinates. The kicker design was optimized for SNS operation, and a detailed simulation study conducted by Holmes [8] showed that two requirements for eigenpainting a Danilov distribution push the limits of these magnets: injection must start with the closed orbit on the foil, both the position and angle of the closed orbit relative to the foil must increase in time. (In practice, amplitude of the  $x$  and  $y'$  bumps dominate, with changes in  $x'$  and  $y$  much smaller giving approximately circular modes.) We increase the available deflection of the kickers for both cases by lowering the energy of the beam from the linac to 800 MeV. We had intended to go to 600 MeV, but issues with the timing system that were not taken into account make this prohibitively difficult. However, upgrades to the kickers to facilitate 1.3 GeV beam after the Proton Power Upgrade [9] were completed early, making 800 MeV experiments viable.

The ring has 44 BPMs, a wall current monitor, and electron profile scanners which are not currently operational, as well as beam loss monitors, and a camera and pyrometer for monitoring the foil. After extraction, the ring beam can also be characterized using five wire scanners in the Ring-Target Beam Transport (RTBT) line, the primary four of which are located in the down-stream section of the line. Each wire scanner has a horizontal, vertical, and diagonal plane. These wire scanners allow reconstruction of the covariance matrix with some tuning of the optics [10].

The only linear coupling elements available in the original SNS design are skew quadrupole correctors. We did not find these magnets sufficient for generating the optics required for these experiments. Experiments done before the installation of sufficient coupling elements are covered in Ref. [11].

### Achieving Coupling

Because the eigenvectors of a solenoid element are circular modes, we can achieve approximately circular modes in

the SNS ring at the injection point by first setting the lattice tunes to be equal, creating degenerate eigenvalues, and introducing a solenoid field. The solenoid breaks the degeneracy, creating distinct counter-rotating modes. The modes will skew but remain elliptical in real-space as they are transported through the lattice. This scheme was suggested in Ref. [12].

Solenoids designed and built by Stangenes Ind. Inc. [13] were added to the ring in late 2022 in a straight section originally intended for a Beam-In-Gap stripline kicker that was never operational, see Fig. 1. The solenoid insert consists of two magnets, shown in Fig. 2, wired in series that provide a total of 0.6 Tm integrated field at 265 A<sup>1</sup>.



Figure 2: Solenoids installed in the SNS ring.

### Measuring Coupling

Tune-up of the machine is done with ‘single mini-pulse’ beam, that is a single turn injection into the ring, injected off-axis. We fit turn-by-turn (TBT) BPM data to measure tunes, and phase and amplitude information. First, we set the ring for equal tunes with no coupling elements energized and verify the tunes. We can reliably set the tunes equal to within  $10^{-3}$ . For these experiments both tunes are set to 6.177.

The solenoids are then turned on, and we verify that the closed orbit is not distorted. TBT BPM data taken with the solenoids on is analyzed for the global parameters: tune, and damping coefficient for each mode using information from all ring BPMs. We use the method outlined by Pelaia [14] extended to a coupled ring to extract this global information. The global fit is done using essentially the function in Eq. (1), but with  $A_{ij}$  and  $\mathbf{v}_{ij}$  combined into a single amplitude coefficient, and no additional phase  $\theta_i$ . This is described briefly in Ref. [15].

For data analysis, the MADX model of the ring is calibrated to reproduce the measured tunes using two parameters: the solenoid-free equal tune value, and the solenoid strength. The solenoid strength sets the tune splitting, and the uncoupled equal tune value sets the absolute values of the

<sup>1</sup> This was erroneously reported as 275 A in Ref. [15]

tunes. We use the PTC module to extract orthonormal eigenvectors from the calibrated model. Each of four eigenvectors has four components, one for each of  $(x, x', y, y')$ . Figure 3 shows the modes described by the calibrated model at the injection location for global parameters:  $\nu_1 = 0.195578$ ,  $\nu_2 = 0.158402$ ,  $\gamma_1 = 0.000144234$ ,  $\gamma_2 = 0.000156413$ . The two vectors describing each mode are indicated by the solid and dashed arrows in the same color.

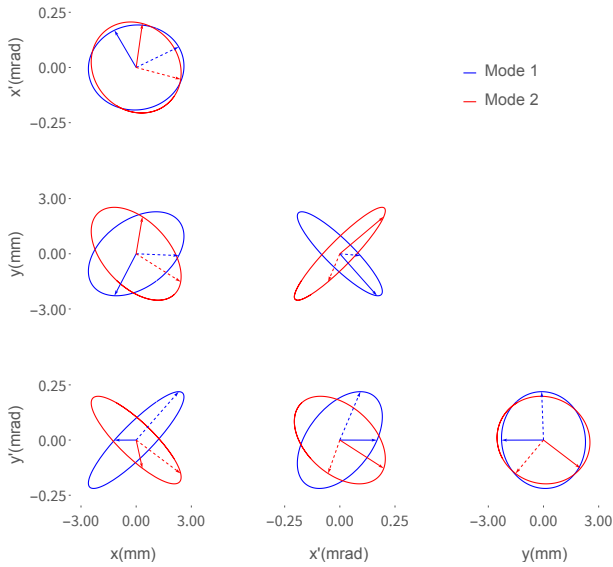


Figure 3: Modes at the foil as predicted by the PTC module of MADX calibrated to the observed tunes. Two vectors for each mode are shown in solid and dashed lines of the corresponding color.

To fit the coupled data, we transport normalized eigenvectors  $\mathbf{v}_{ij}$  from the foil to each of the BPMs in the ring and then fit all BPMs for the amplitude and phase of each mode,  $A_1, A_2, \theta_1, \theta_2$ , (transporting the vectors to each BPM is equivalent to adding a term to the oscillatory functions for the phase advance to each BPM):

$$\begin{aligned} \mathbf{x}_{\text{BPM}}(n) = & e^{-\gamma_1 n^2} A_1 (\mathbf{v}_{11, \text{BPM}} \cos(\phi_1(n) + \theta_1) \\ & + \mathbf{v}_{12, \text{BPM}} \sin(\phi_1(n) + \theta_1)) \\ & + e^{-\gamma_2 n^2} A_2 (\mathbf{v}_{21, \text{BPM}} \cos(\phi_2(n) + \theta_2) \\ & + \mathbf{v}_{22, \text{BPM}} \sin(\phi_2(n) + \theta_2)) + f, \end{aligned} \quad (1)$$

where the bold symbols represent 4D vectors in  $(x, x', y, y')$ , and  $\phi_i(n) = 2\pi\nu_i n$ ,  $n$  is the turn number,  $\gamma, \nu$  are damping rate, and tune determined by the model calibrating global fit. Fitting TBT data requires taking the  $x, y$  components as necessary. Formulating the fit in this way means that the amplitude and phase are both global values, with  $\mathbf{v}_{ij}$  containing information about the 4D Twiss functions. The corresponding emittance for each mode is simply  $\varepsilon_i = A_i^2$ . Implicit in this fit is the assumption that damping is not significant over a single turn, which is reasonable with measured damping rates  $\gamma_i \approx 10^{-4}$ .

Figures 4 and 5 show the result of this fitting procedure on TBT data for a case injecting onto arbitrary coordinates, and one optimized for single mode injection respectively. The data shown are from BPM B01 at the beginning of the first arc, but the fits were done globally. The contribution from each mode is plotted on the same images as dashed lines for comparison. For the two cases shown in Figs. 4 and 5 the corresponding fit parameters are given in Table 1.

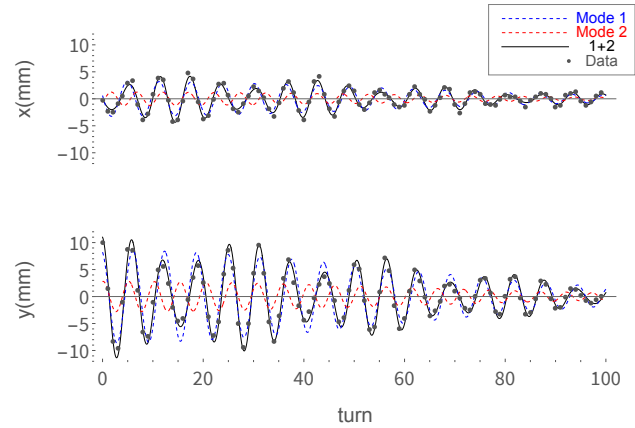


Figure 4: TBT data with fit for injection with significant amplitude for both modes.

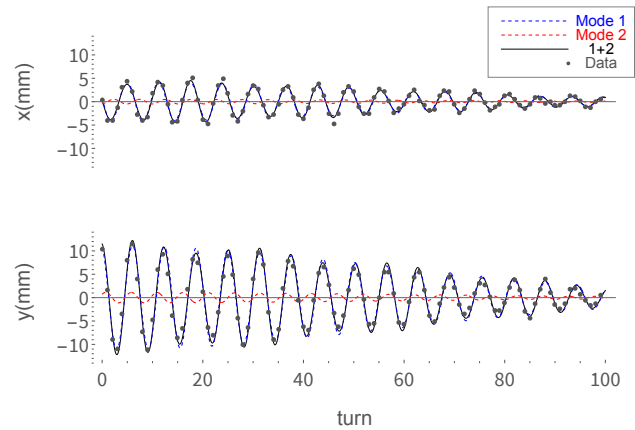


Figure 5: TBT data with fit for injection primarily into one mode.

Table 1: Eq. (1) TBT Fit Results

Parameter	Arbitrary Inj.	Single Mode
$A_1 (\sqrt{\text{mm mrad}})$	$3.22 \pm 0.010$	$4.19 \pm 0.012$
$\theta_1$	$0.150 \pm 0.0005$	$0.148 \pm 0.0004$
$A_2 (\sqrt{\text{mm mrad}})$	$1.16 \pm 0.010$	$0.46 \pm 0.012$
$\theta_2$	$0.432 \pm 0.001$	$0.320 \pm 0.004$
$\frac{\varepsilon_1}{\varepsilon_2} = \left(\frac{A_1}{A_2}\right)^2$	$7.71 \pm 0.14$	$80.37 \pm 4.00$

The single-mode injection case above was achieved by first injecting into approximately correct coordinates generated by the linear model prior to the experiment, without

calibration, and then hand tuning the injection to minimize the second mode. We first maximized the angular kick  $y'$ , and then tuned the size of the bump in  $x$  to achieved optimal results. This procedure will be modified in future experiments to make use of the calibrated model. Each mode has two associated 4D vectors, for a total of 4 vectors specifying  $(x, x', y, y')$ . Using the two vectors describing the evolution of one mode we find the optimal phase. We search for the phase such that the  $x$  and  $y'$  components maximized as simulation showed this was the optimal phase for beam loss and kicker utilization. The linear model of the ring in the OpenXAL model is used to change the kicker strengths to produce the desired coordinates at the foil.

One complication is that the OpenXAL model used for online beam control does not currently contain a well-tested description of the solenoids. However, because we have verified that there is no effect on the closed orbit, the solenoids can be turned off when modifying and measuring the closed orbit parameters, and re-energized to verify the effect on beam. In the future, the online model will be updated to include the solenoids, but the method described here produces reasonable, repeatable results.

The ratio of the mode emittances, shown in the last line of Table 1, represents one factor determining the upper limit on the achievable emittance ratio in the painted beam, therefore it is crucial that the ratio be as large as possible before painting. The dimensions of the linac beam, or the ‘size of the paintbrush’ projected onto the eigenvectors of the ring, mismatch due to space charge (not captured in the TBT analysis), and any other sources of small-mode heating all also contribute to a reduced emittance ratio after painting.

### Eigenpainting

To fill an elliptical mode requires increasing the amplitude of a vector lying in the plane defined by the two vectors. To fill it uniformly requires increasing the amplitude as the square root of time, such that fixed-size pulse from the linac is allowed to fill the increasingly larger area described by the motion around subsequently larger ellipses enclosing the previously injected beam.

The initial point for painting is given by the kicker settings such that the beam is injected on the closed orbit, and the final point is given by the coordinates determined by minimizing the small-mode component. The single-mode injection case presented above is the end point for painting in the following.

Painting is then accomplished by drawing a kicker waveform from the initial set of kicker voltages to the final set. Typical painting waveforms for eigenpainting are shown in black in Fig. 6. The pink dashed lines indicate the production waveforms. Kickers 1 and 2 are upstream of the foil, and 2 and 4 are downstream, in both planes.

### Measuring Painted Beam

The process of measuring the 4D emittance in the SNS RTBT is described in detail in Ref. [10]. The procedure is time consuming, requiring accumulation and extraction for

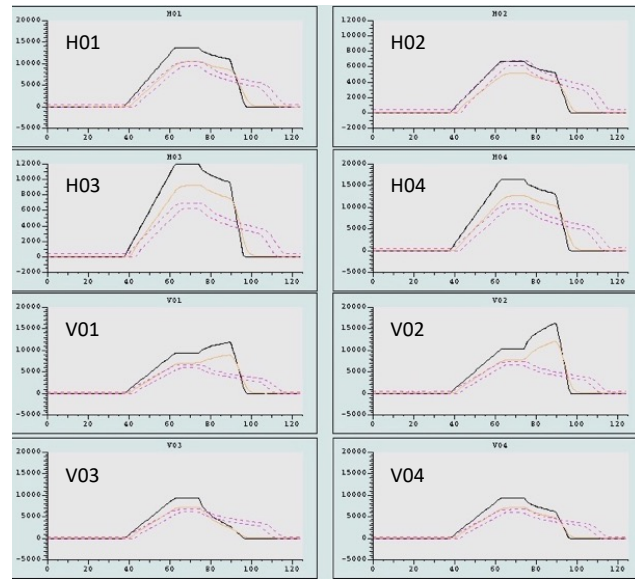


Figure 6: Horizontal (H) and Vertical (V) kicker waveforms for eigenpainting (black), pink envelope shows production waveforms.

every point in the profile. At the low repetition rate needed for these studies, it takes about 5 minutes to get one set of wirescans. Two sets with different RTBT optics are required for a reliable reconstruction. Beyond a certain point, it is necessary to include space charge in the match [16] for the distribution. This can be done in simulation, but there is no measurement fast enough using the diagnostics available to provide a reliable metric for optimization of painting parameters. In this case we are entirely dependent on simulation to provide guidance for the correction of eigenvectors in the presence of space charge. No such correction has yet been implemented.

However, electron scanners in the SNS ring are currently being upgraded. Though they will not provide full 4D information, we hope to use these scanners to get a quick assessment of the profile quality, and possibly use them to optimize painting in the presence of space charge by examining the time-evolution of the profiles during extended storage.

The wirescans in the RTBT provide profiles and a reconstruction of the 4D emittances, which can be used to determine the emittance ratio of the painted beam. The emittance ratio is the ultimate figure of merit for many applications of circular modes, and by extension the Danilov distribution, with larger values indicating better population of the desired mode. (For convenience we always express the ratio with the larger emittance in the numerator.) Because of the uniform distribution of charge, and the elliptical envelope of a Danilov distribution, 1D profiles should be half-ellipses, which is easy to verify with wirescanners.

Figure 7 shows the wirescans at the end of accumulation for an experiment that included solenoids. A complete analysis of these experiments is in progress and will be published

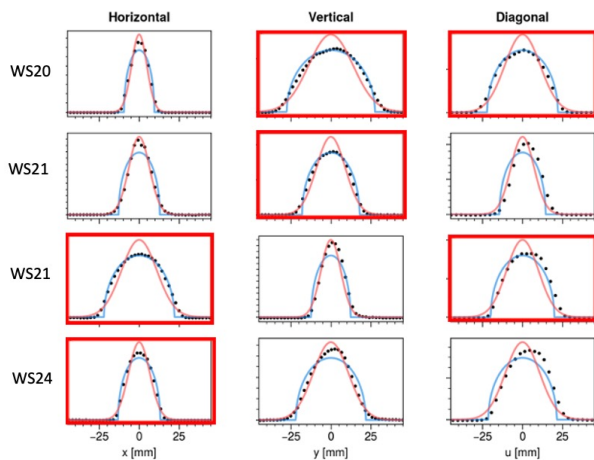


Figure 7: RTBT wirescans of painted optimized beam. A Gaussian (red) and elliptical (blue) fit are overlaid. Profiles showing more elliptical shape are highlighted.

at a later date. However, note that two fits have been applied to the data, a Gaussian fit, and a semi-elliptical, in several select projections highlighted in red the elliptical fit is very convincing. To some extent this difference in projections is expected from Ref. [8]. For the projections which deviate from elliptical we suspect, but have not confirmed, that the projection is dominated by the non-zero emittance from the second mode. A more detailed analysis will address this with comparison to simulation.

## STATUS AND OUTLOOK

We have achieved our initial goal of developing a procedure for eigenpainting into a ring, and are currently preparing a detailed analysis of the resulting experiments. We have identified several opportunities for improvement at SNS.

Painting experiments at the SNS are time consuming because of the setup time for low energy beam. While it is easy to stop accelerating early in the linac, modifying the ring clock which drives the chopper that determines the minipulse structure causes issues with modulators that have to be addressed. This is not a fundamental limitation, and efforts are being made to address the long setup time, which could greatly increase the productivity of future experiments.

The 4D emittance measurements are also time consuming, requiring at least two separate sets of optics in the RTBT for reliable results. Each scan takes roughly 5 minutes. The electron profile scanners in the ring would provide a viable real-time look at profiles. They are not currently available as upgrades are underway. Even so, the electron scanners will not be able to provide a full 4D phase space measurement, but they will allow turn-by-turn monitoring of the profiles and the feedback they provide may be sufficient for quickly optimizing an approximately correct setup.

We plan to carry out more extensive studies of the properties of Danilov distributions, and circular modes more generally, with particular interest in the long-term behavior of these distributions as a function of space charge, and near

resonances. To-date a very preliminary study was conducted to drive the coupled eigenmodes onto resonance using the solenoid.

With eigenpainting established, we can also probe the difference between a circular mode with a Gaussian distribution in the large emittance mode, and the Danilov distribution. Not restricting ourselves to the Danilov distribution, we can consider experiments at higher energy, but we will not be able to inject at the center of the distribution, similar to SNS production painting.

There are many issues that need to be resolved regarding the reality of Danilov distributions mentioned here, e. g.: Does the possibly helpful reduced tune spread lead to other issues of stability from lack of damping? How compact a tune footprint is achievable in reality? Are the drivers of small-mode heating sufficiently weak to allow accumulation and acceleration without special consideration? Does the reduction of non-linear space charge reduce halo formation, if so, what is the scale of the improvement? What modifications would need to be made to downstream machines to ensure beams suitable for a given application, say, a collider or high-power proton driver?

## CONCLUSION

The Danilov distribution offers a unique opportunity to explore the consequences of linear space charge in a scalable way in existing accelerators with very little modification. Because the linear nature of the space charge simplifies theoretical considerations, these distributions are ideal for probing questions about stability, space charge limits, and halo formation experimentally.

We outlined several of the high-level arguments for possible benefits of Danilov distributions, and circular modes, or rotating beams more generally, as presented in the literature.

We also outlined the procedure developed at SNS to inject into a single elliptical mode with a flexible phase space painting system.

## ACKNOWLEDGMENTS

This work would not be possible without the help of many people across SNS too numerous to list. Particular thanks to Charles Peters and Dave Brown. This work was supported by UT-Battelle, LLC, under Contract No. DE-AC05-00OR22725 with the U.S. Department of Energy, and Field Work Proposal ORNL-ERKCS41-Funding.

## REFERENCES

- [1] V. Danilov *et al.*, “Self-consistent time dependent two dimensional and three dimensional space charge distributions with linear force”, *Phys. Rev. Spec. Top. Accel. Beams*, vol. 6, p. 094204, 2003. doi:10.1103/PhysRevSTAB.6.094202
- [2] I. M. Kapchinsky and V. V. Vladimirsky, “Limitations of proton beam current in a strong focusing linear accelerator with the beam space charge”, in *Proc. HEACC’59*, CERN, Geneva, Switzerland, Sep. 1959, pp. 274–287.

- [3] O.J. Liuten *et al.*, “How to realize uniform three-dimensional ellipsoidal electron bunches”, *Phys. Rev. Lett.*, vol. 93, p. 094802, 2004.  
doi:10.1103/PhysRevLett.93.094802
- [4] A. Burov, “Circular modes for flat beams in the LHC”, *Phys. Rev. Spec. Top. Accel. Beams*, vol. 16, p. 061002, 2013.  
doi:10.1103/PhysRevSTAB.16.061002
- [5] A. Burov *et al.*, “Circular modes, beam adapters, and their applications in beam optics”, *Phys. Rev. E*, vol. 66, p. 016503, 2002. doi:10.1103/PhysRevE.66.016503
- [6] Y.-L. Cheon *et al.*, “Mitigation of space-charge-driven resonance and instability in high-intensity linear accelerators via beam spinning”, *Nucl. Instrum. Methods Phys. Res., Sect. A*, vol. 1013, p. 165647, 2021.  
doi:10.1016/j.nima.2021.165647
- [7] D. Raparia, “SNS injection and extraction devices”, in *Proc. PAC’05*, Knoxville, TN, USA, May 2005, paper TOAA007, pp. 553-557.
- [8] J. Holmes *et al.*, “Injection of a self-consistent beam with linear space charge force into a ring”, *Phys. Rev. Accel. Beams*, vol. 21, p. 124403, 2018.  
doi:10.1103/PhysRevAccelBeams.21.124403
- [9] J. Galambos *et al.*, “Proton power upgrade final design report”, ORNL, Oak Ridge, TN, USA, Rep. ORNL/TM-2020/1570, 2020. doi:10.2172/1784163
- [10] A. Hoover and N. J. Evans, “Four-dimensional emittance measurement at the Spallation Neutron Source”, *Nucl. Instrum. Methods Phys. Res., Sect. A*, vol. 1041, p. 167376, 2022.  
doi:10.1016/j.nima.2022.167376
- [11] A. Hoover, “Towards the production of a self-consistent phase space distribution”, PhD thesis, University of Tennessee, Knoxville, TN, USA, 2022.  
[https://trace.tennessee.edu/utk\\_graddiss/7228](https://trace.tennessee.edu/utk_graddiss/7228)
- [12] J. Holmes *et al.*, “Painting self-consistent beam distributinos in rings”, in *Proc. PAC’05*, Knoxville, TN, USA, May 2005, paper TPAT031, pp. 2194–2196.  
doi:10.1109/PAC.2005.1591054
- [13] Stangenes Industries Inc. <https://www.stangenes.com>
- [14] T. Pelaia II, “Parameter estimation of Gaussian-damped sinusoids from a geometric perspective”, 2016.  
doi:10.48550/arXiv.1604.05167
- [15] N. J. Evans *et al.*, “Phase space painting of a self-consistent Danilov distribution in the SNS ring”, in *Proc. IPAC’23*, Venice, Italy, May 2023, pp. 2483–2486.  
doi:10.18429/JACoW-IPAC2023-TUPM115
- [16] A. Hoover *et al.*, “Computation of the matched envelope of the Danilov distribution”, *Phys. Rev. Accel. Beams*, vol. 24, p. 044201, 2021.  
doi:10.1103/PhysRevAccelBeams.24.044201